September 2002

Fault detection for salinity sensors in the Columbia Estuary

Cynthia Archer

Antonio Baptista

Todd K. Leen

Fault Detection for Salinity Sensors in the Columbia Estuary

Cynthia Archer, Antonio Baptista, Todd K. Leen
OGI School of Science and Engineering
Oregon Health and Science University

September 20, 2002

Abstract

Sensors deployed in the Columbia River estuary gather information on physical dynamics and changes in estuary habitat. Of these sensors, conductivity sensors are particularly susceptible to bio-fouling, which gradually degrades sensor response and corrupts critical data. Several weeks may pass before degradation is visibly detected. As a result, an indeterminate amount of the archival data is corrupted, as the onset time of bio-fouling is unknown. To speed detection and minimize data loss, we develop automatic bio-fouling detectors, based in machine learning approaches, for these conductivity sensors. We demonstrate that our detectors identify bio-fouling at least as reliably as human experts and provide accurate estimates of bio-fouling onset time. Real-time detectors installed during the summer of 2001 produced no false alarms, yet detected all episodes of sensor degradation before the field staff.

1 The Bio-fouling Problem

Environmental observation and forecasting systems (EOFS) gather, process, and deliver environmental information to facilitate sustainable development of natural resources. Our work is part of a pilot EOFS system being developed for the Columbia River Estuary (CORIE) [1, 2, 3]. This system uses data from sensors deployed throughout the estuary (Figure 1) to calibrate and verify numerical models of circulation and material transport. CORIE scientists use these models to predict and evaluate the effects of development on the estuary environment [4].

CORIE salinity sensors deployed in the harsh estuary environment lose several months of data every year due to sensor degradation. As an example of the severity of the problem, degradation of salinity sensors is so common in late summer that the data archive contains little or no reliable salinity data for the beginning of the rainy season. Corrupted and missing field measurements compromise model calibration and verification. This in turn can lead to invalid environmental forecasts and erroneous conclusions about effects of development on the estuary environment.

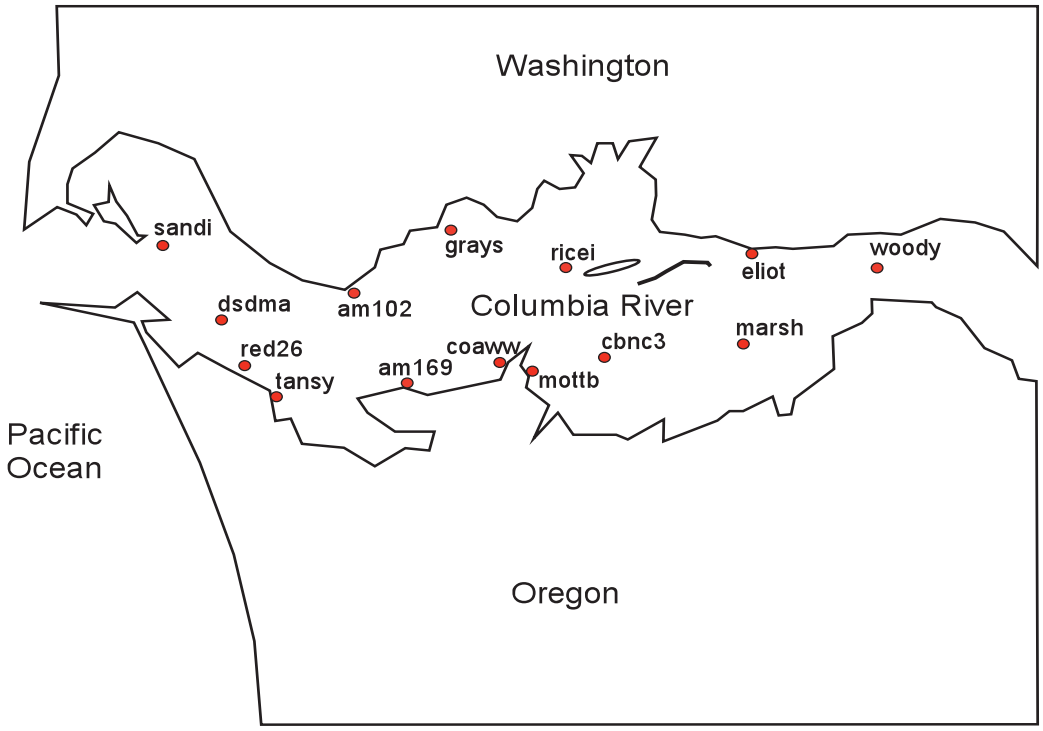

Figure 1: Map of the Columbia River estuary marked with approximate locations of CORIE sensor stations

A common yet particularly insidious form of salinity sensor degradation is bio-fouling. Bio-

fouling occurs when biological matter accumulates on the sensors, reducing their responsiveness. Field staff do not have time to study the sensor measurments every day searching for this gradual degradation. Consequently, the bio-fouling process goes undetected for weeks or months until a sensor becomes substantially compromised. Even after sensor failure is visually obvious, the precise onset time of bio-fouling remains uncertain, leaving a history of unreliable measurements.

Early bio-fouling detection is made difficult by the normal variability of salinity measurements. Tides cause the measurements to vary from river salinity to near ocean salinity twice a day. In addition, the patterns of salinity measurements are different for every station. For instance, sensors near the mouth of the estuary measure higher salinity at tidal flood than do sensors further up-river. Changes in weather and ocean condition cause additional variations in salinity. To complicate bio-fouling detection further, the bio-fouling signature also varies from episode to episode.

To improve the integrity of CORIE system data, we must accomplish two objectives. First, we must detect bio-fouling quickly (within several diurnal cycles). This early detection will limit the use of corrupted data in real-time or on-line applications. Second, we must estimate the onset time of bio-fouling. Having an estimate of onset time will allow us to remove corrupted measurements from the data archive. In this work, we concentrate on developing automatic classification systems to detect bio-fouling of conductivity sensors used to measure salinity.

2 Characterizing Sensor Bio-fouling

Salinity is a measure of the mass of dissolved salts in one kilogram of water (g/kg) and is expressed in practical salinity units (psu). The CORIE systems includes several inductive conductivity and temperature (CT) sensors deployed in the estuary. Salinity is determined from the electrical conductivity of the water with corrections for temperature and pressure at the sensor site [5].

A CT sensor reports reduced salinity when it bio-fouls. The sensor measures the conductivity of a calibrated volume of water. Biological material accumulating on the sensor fills the measurement cavity, reducing the actual volume of water measured. Consequently, the reported salinity is lower than the true salinity. Once bio-fouling begins, degradation increases until biological material fills the cavity and then levels off. The degradation rate

and final degradation level differs for every bio-fouling incident.

We observe two types of bio-fouling in the estuary, hard-growth and soft-growth. Hard-growth bio-fouling is primarily caused by barnacles growing on the sensors. Barnacles are primarily found on sensors close to the ocean where maximum tidal salinity is high. It is characterized by linear degradation until the barnacles fill the sensor measurement cavity. Soft-growth bio-fouling is caused by plant material growing on and around the sensor. It is characterized by by slow linear degradation with occasional interruptions in the downtrend. In addition, the sensor response partially recovers in the winter months, presumabley due to plant material die back. In either case, the time from onset to complete bio-fouling takes anywhere from 3 weeks to 5 months.

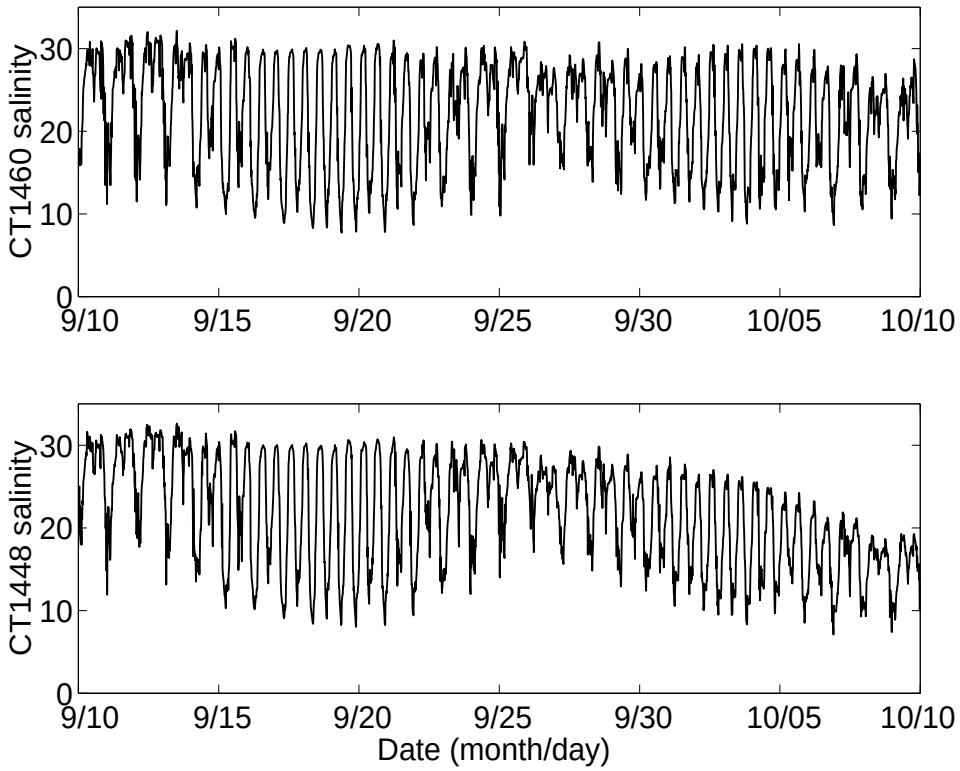

Figure 2: Clean and bio-fouled salinity time series examples from Red26 station. The upper time series os from clean instrument CT1460. The lower time series from instrument CT1448 shows degradation beginning on September 28, 2001. On removal, CT1448 was found to be bio-fouled.

Figure 2 illustrates both tidal variations in salinity and the effect that bio-fouling has on these measurements. It contains salinity time series from two sensors mounted at the Red26 station, Figure 1. The upper trace, from midwater mounted sensor CT1460, contains only

clean measurements. The lower trace, from riverbed mounted sensor CT1448, contains both clean and bio-fouled measurements. The first half of the two time series are very similar, but beginning on September 28^{th}, the salinity measurements diverge. The deeper sensor, CT1448, exhibits the degradation typical of hard-growth bio-fouling.

3 Evaluation Bio-fouling Detectors

Previously, no automatic classification system existed for detecting sensor bio-fouling. In our context, an automatic classifier distinguishes between signals from clean and bio-fouled sensors. Prior to this work, bio-fouling was identified by visually examining the salinity time series. When the salinity was lower than expected for several weeks, the sensor was declared bio-fouled. Since no automatic classification system exists, we first develop two baseline classifiers using standard statistical pattern recognition techniques. However, these baseline classifiers do not provide estimates of bio-fouling onset time. Consequently, we also develop two new classifiers, based on sequential likelihood ratio tests, that provide early bio-fouling detection and onset time estimates. Before discussing these classifiers, we describe the data used in our evaluations and the method we employ to evaluate classifier performance.

3.1 Evaluation Data

We evaluated our bio-fouling detectors on measurements from CORIE salinity sensors predominantly subject to hard-growth bio-fouling. Hard-growth bio-fouling is of particular interest in this initial work, as human experts typically identify this type within 15 days of onset and can estimate the onset time with reasonable certainty. Due to the slow and variable nature of soft-growth bio-fouling, it is less amenable to human identification until it has progressed to an advanced stage. The accuracy with which human experts identify hard-growth bio-fouling sets a high standard for our automatic classifiers.

The results presented in this paper are from two of the tested stations. The first sensor is mounted at Sand Island, labeled "sandi" in Figure 1, which is the station closest to the ocean. It is subject to only hard-growth bio-fouling and has the most consistent salinity measurements of all the estuary stations. The second sensor is mounted at Tansy Point, labeled "tansy" in Figure 1, and is subject to both hard-growth and soft-growth bio-fouling.

This station is further up-river than Sand Island, so the salinity measurements show greater sensitivity to changes in tidal strength and river flow. This greater variability in both salinity and bio-fouling behavior makes bio-fouling detection more challenging at Tansy Point than at Sand Island.

Our evaluation data includes time series segments from the CORIE data archive as well as measurements gathered during the summer of 2001. Bio-fouling is most prevalent during the summer period of mid-April to mid-October, so we limit our evaluation to this time period. We have four time-series segments for Sand Island and three segments for Tansy Point. Figure 3 contains the latter part of the summer 2000 time series for these stations. Both these segments exhibit degraded measurements due to bio-fouling. For all the sensor data used in our evaluation, bio-fouling was previously verified by removing and inspecting the sensor. Bio-fouling onset time is unknown, so we estimated it visually with the assistance of our field scientist.

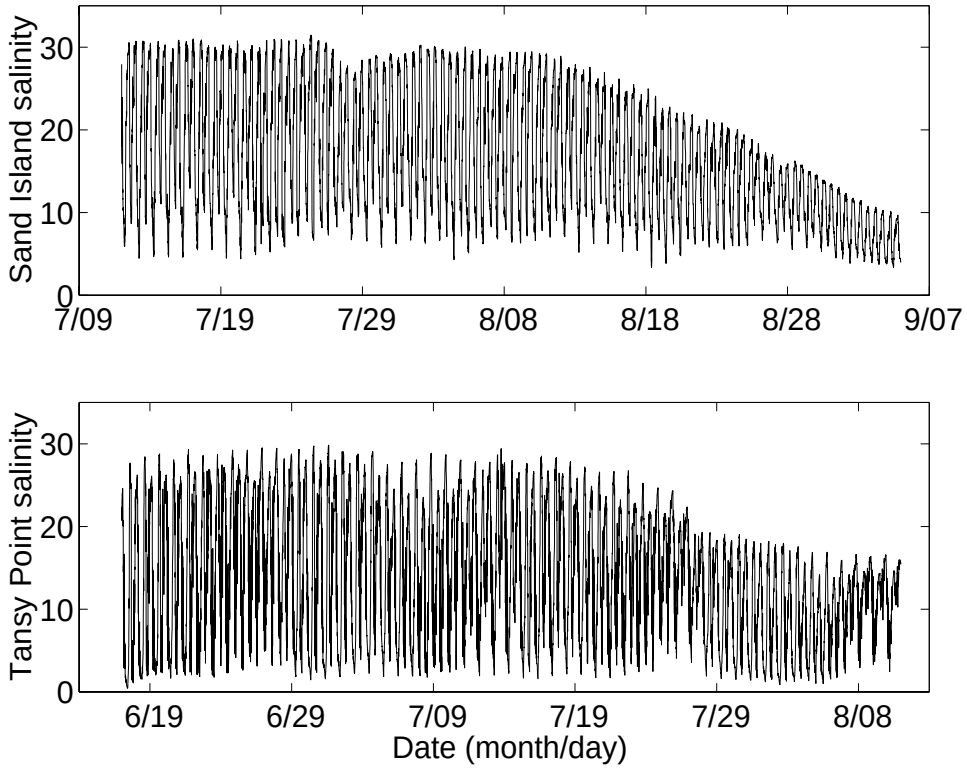

Figure 3: Segments of bio-fouled salinity time series from Sand Island (top) and Tansy Point (bottom) stations taken from summer 2000 data archive. Estimated bio-fouling onset time for Sand Island is August 11 and for Tansy Point is July 17.

3.2 Evaluating Classifier Performance

To evaluate classifier performance, we use receiver operating characteristics (ROC). An ROC provides the information to assess detector performance for any cost function. It plots percentage of false alarms (identify clean signal as bio-fouled) against percentage of correct detections (identify bio-fouled signal as bio-fouled) for a range of detector threshold values. We are interested in detection at low false alarm rates. Replacing instruments is expensive in terms of time and resources. Consequently, we want to be confident that a sensor is bio-fouled before sending a diver out to retrieve and replace it.

To accurately characterize classifier performance we must use our small data set effectively. There are too few examples to divide the data into fixed development (training) and test sets. Instead we generate two ROC curves for each classifier using resubstitution and hold-out methods. For resubstitution, the classifier is developed and tested on all the available data. This method gives somewhat optimistic estimates of classifier performance. For hold-out, we develop a series of classifiers. Each classifier is trained using all but one of the example time-series segments and is tested on the held-out segment. Each time series segment is held-out in turn. The results from these classifiers are combined to form a single ROC, which gives a more conservative estimate of classifier performance. Expected classifier performance will lie between these two curves [6].

4 Baseline Methods for Bio-fouling Detection

When we began this work, no automatic classification system existed for detecting sensor bio-fouling. As a starting point, we developed two baseline classifiers using standard statistical pattern recognition techniques. This section describes these baseline classifiers and their performance on CORIE test data. The first classifier monitors only salinity measurements and indicates whether or not the sensor is bio-fouled. The second classifier monitors both salinity and temperature measurements to improve bio-fouling detection and reduce false alarm rates.

4.1 Classification with Maximum Diurnal Salinity

Our first task involved identifying candidate input features for the classifiers. A useful classification feature shows a large shift in value when the sensor is bio-fouled, but has low variability when the sensor is clean. Maximum diurnal (md) salinity, defined as the maxi-

mum salinity over two tidal periods, satisfies these criteria. When the sensor is clean, the md salinity stays close to some mean value, with occasional dips of several psu presumably precipitated by changing ocean and river conditions. When the sensor bio-fouls, the md salinity gradually decreases to typically less than half its normal mean value, as seen in the Figure 3 examples. The rate of bio-fouling varies with each incident. Once bio-fouling begins, a sensor progresses from clean to fully degraded in 20 to 150 diurnal cycles.

To extract the md salinity feature, we first need to know the times of tidal ebb and flood. The pressure sensor at each station is immune to bio-fouling, providing us with reliable tidal information. The times of tidal ebbs are determined by finding minimums in the pressure signal. We then find the maximum salinity between the times of each pair of tidal ebbs. This is the tidal maximum salinity. One tide of each pair will be stronger, resulting in higher salinity values. The maximum *diurnal* salinity is the larger of each pair of tidal maximum salinities. Figure 4 illustrates feature extraction.

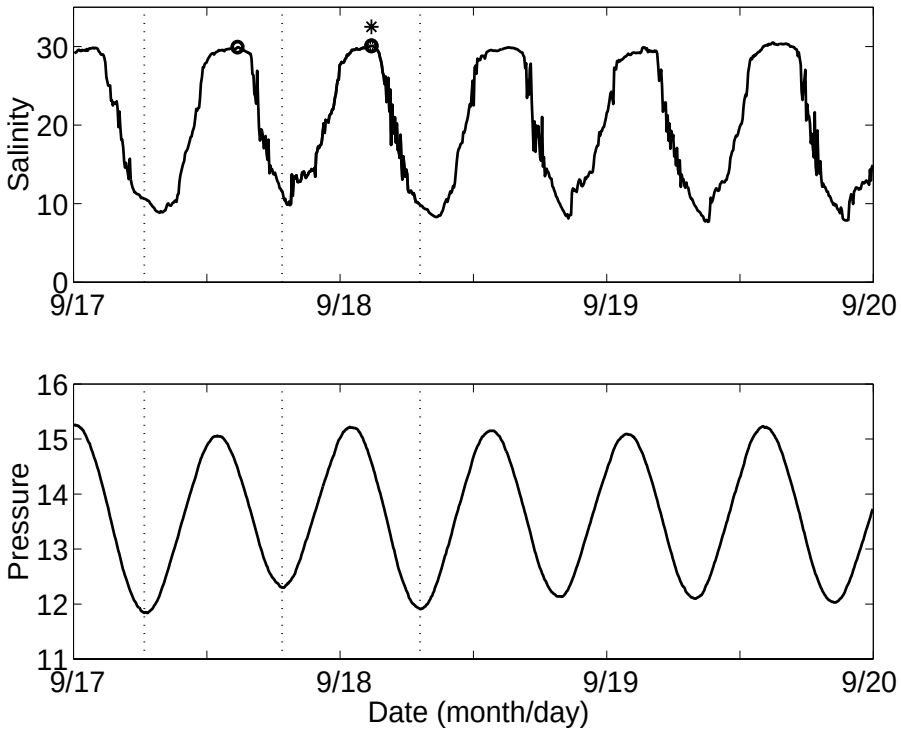

Figure 4: Segment of salinity and pressure time series demonstrating extraction of maximum diurnal salinity. First, we identify tidal ebbs, marked with dotted lines. Then, we find maximum salinity between each pair of ebbs, marked with $\circ$. The maximum diurnal salinity is the higher of the pair of tidal maximums (29.91 and 30.08), marked with $*$.

Md salinity, s, behaves as if it has some constant level, μ_s, but is perturbed by noise, ϵ, that is

$$s = \mu_s + \epsilon \tag{1}$$

If the noise ϵ is Gaussian with zero mean and variance of σ_s^2, the probability density of s is also Gaussian, $\mathcal{N}(\mu_s, \sigma_s^2)$, that is

$$\mathrm{p}(s) = \frac{1}{\sqrt{2\pi}\sigma_s} \exp \frac{-(s-\mu_s)^2}{2\sigma_s^2} \tag{2}$$

Figure 5, which shows a histogram of measured salinity from a clean sensor at Tansy Point, demonstrates that this Gaussian assumption, while not perfect, is not unreasonable. We plan to develop more accurate density models in future work.

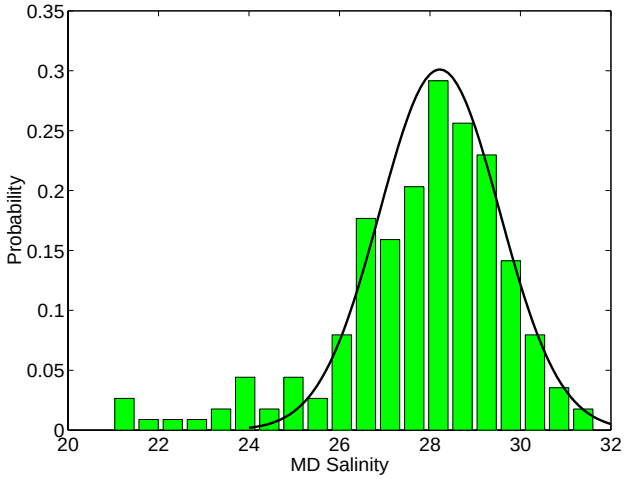

Figure 5: Histogram of clean sensor salinity measurements from Tansy Point. A Gaussian distribution, fit to the mean and variance of the data, is shown in black. The data matches this curve well except for a few low salinity points. We see occasional short periods of low salinity apparently related to increases in river flow.

When the sensor bio-fouls, the measurement at time n, x_n, will be less than the true salinity, s_n. Consequently, the expected residual $\mathsf{E}[x_n - \mu_s]$ will be zero when the sensor is clean and negative when the sensor is bio-fouled. To use maximum diurnal salinity to identify bio-fouling, we compare the residual $x_n - \mu_s$ to a threshold. If the residual is below the threshold, the sensor is identified as bio-fouled. The performance of md salinity classifiers developed for and applied to Sand Island and Tansy Point data are shown in Figure 6. Resubstitution and hold-out results are similar. For near zero false alarm rate (never classify a clean example as bio-fouled), these classifiers correctly identify roughly 65% of the Sand Island and less than 30% of the Tansy Point bio-fouled days. At 5% false alarm, the percent correct identification increases to 80% and nearly 50% respectively.

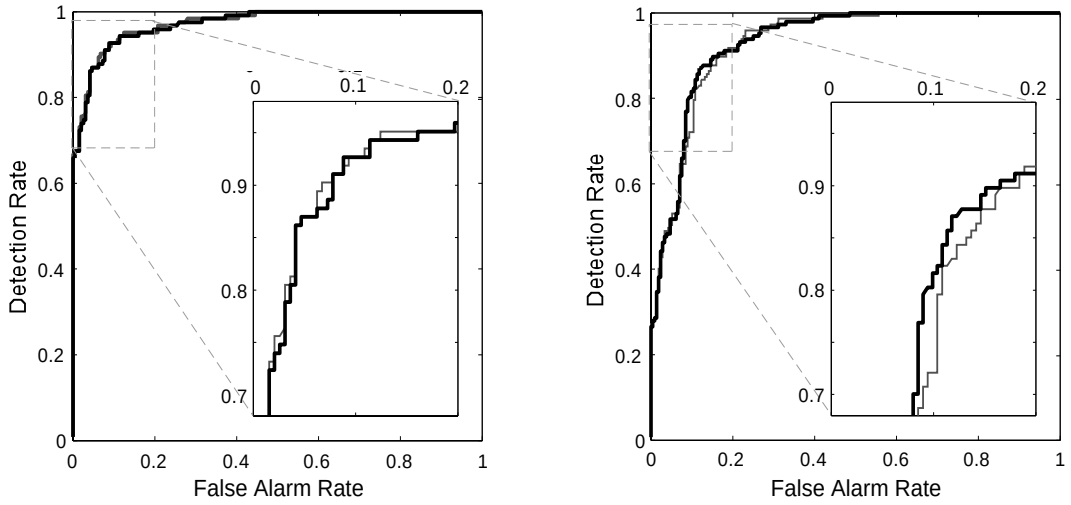

(a) Sand Island

(b) Tansy Point

Figure 6: Maximum Diurnal Salinity resubstitution (thin line) and hold-out (thick line) ROC for classification of Sand Island and Tansy Point data.

4.2 Incorporating Temperature to Reduce False Alarms

Classifiers that monitor salinity alone can not distinguish natural decreases in salinity from early bio-fouling. An example of a natural salinity decrease is apparent in the top plot, Figure 3, around July 25. The low salinity measurements below the main Gaussian bump in Figure 5 are presumed to be due to *natural* changes in ocean and river conditions. Natural salinity decreases can be recognized, if we can examine a correlated source of uncorrupted information, such as a nearby clean sensor or a sensor measuring a related value. The temperature sensor included with each conductivity sensor is not subject to bio-fouling. Consequently, we can use temperature measurements as a correlated and uncorrupted source of salinity information.

The salinity and temperature at a station are products of the same mixing process of ocean and river waters, so we expect the values at tidal flood will be correlated. To show this, we assume a standard linear mixing of ocean and river waters. The measured salinity S_m and temperature T_m at a station are then linear functions of ocean values $\{S_o, T_o\}$ and river values $\{S_r, T_r\}$

$$S_m = \alpha(t)S_o + (1 - \alpha(t))S_r \tag{3}$$

$$T_m = \alpha(t)T_o + (1 - \alpha(t))T_r \tag{4}$$

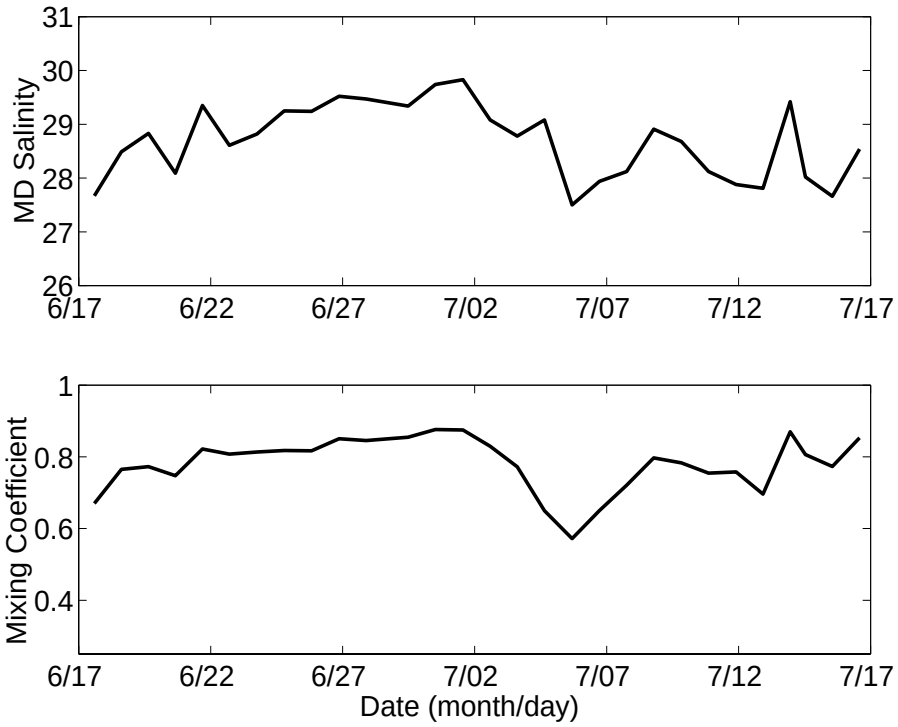

Figure 7: Time series of md salinity and temperature-based mixing coefficient values showing the correlation between salinity and temperature measurements. Data from Tansy Point, summer 2000.

where $\alpha(t)$ is the mixing coefficient at time t and river salinity S_r is close to zero. We focused our work on the late spring through summer period when bio-fouling is most prevalent. In this period the temperature is anti-correlated with salinity, $T_o < T_r$. The estimated mixing coefficient

$$\alpha(t) = \frac{T_r - T_m}{T_r - T_o} \tag{5}$$

will be well correlated with salinity, $S_m \approx \alpha S_o$. Figure 7 contains time series of salinity and the temperature based mixing coeffcient from Tansy Point that show this correlation. We estimate the ocean temperature to be a $T_o = 8°\mathrm{C}$, based on minimum temperatures seen at the outermost sensor station (Sand Island). The river temperature, T_r, is estimated from the station temperature at the tidal ebb, which generally agrees with temperature measurements from upriver stations.

Given the correlation of temperature and salinity, we now develop a classifier dependent on this relationship. We use the well-known technique of Fisher Linear Discriminant Analysis (LDA) [7] as a starting point. Pairs of temperature-based mixing coefficient values, α, and md salinity, s, form a 2-dimensional data vector, x. Fisher LDA defines a projection

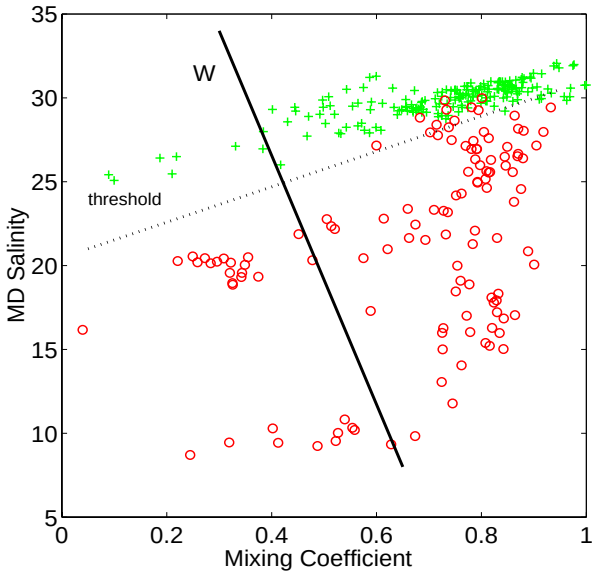

Figure 8: Scatterplot of clean and bio-fouled data from Sand Island showing the relationship between maximum diurnal salinity and temperature-based mixing coefficient. Clean samples are indicated by + and Bio-fouled samples by a ∘. An example transform W projects the data onto the black line and the dotted line indicates an example threshold. Values below the threshold are considered to be from a bio-fouled sensor.

operator, W, that reduces such multi-dimensional data to a scalar while maximizing the separation between data from two classes. This transform is given by

$$W = \Sigma^{-1}(\mu_c - \mu_f) \tag{6}$$

In our case, μ_c and μ_f are the means of the clean and bio-fouled data examples and Σ is the sum of the clean and bio-fouled data covariance matrices. A classifier based on Fisher LDA monitors the discriminant, $h = W^T x$. The discriminant h is tested against a threshold to decide whether or not the signal is bio-fouled. Figure 8 is a scatterplot of temperature-based mixing coefficient and md salinity from Sand Island that shows one possible transform and threshold. Values below the threshold are classified as bio-fouled and values above the threshold are classified as clean.

We evaluated our Fisher LDA based classifiers on the CORIE test data. Figure 9 shows ROC curves for these classifiers in black; the previous salinity alone results are shown in gray. At a given false alarm rate, the Fisher LD generally labels more bio-fouled examples correctly than does the salinity alone feature. For instance, at near zero false alarm rate, correct bio-fouling classification at Tansy Point doubles from less than 30% to between 60% and 70%. The exception in performance improvement is the hold-out curve for Sand Island.

In this case, one of the hold-out training sets had too few bio-fouled measurements for robust classfier development. The poor hold-out results at Sand Island illustrate the importance of having enough representative data to estimate classifier parameters accurately.

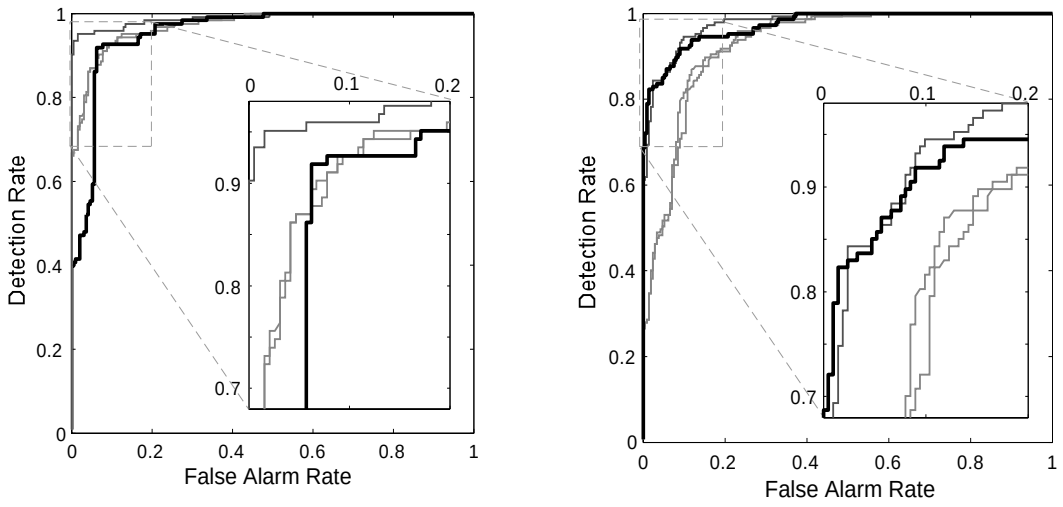

(a) Sand Island

(b) Tansy Point

Figure 9: Fisher linear discriminant resubstitution (thin line) and hold-out (thick line) ROC for classification of Sand Island and Tansy Point data. Maximum diurnal salinity results are underlaid in gray.

5 Limitations of Baseline Methods

Our baseline classifiers have several limitations. Neither method provides an estimate of bio-fouling onset time. Developing the Fisher LDA based classifier requires many examples of bio-fouling, which are not available. Both methods operate on a single measurement at a time, yet bio-fouling is a progressive process. We expect that combining information from several sequential measurements will improve classifier accuracy.

A critical missing element for our task is the lack of onset time estimate. Since bio-fouling is a gradual process, data before the bio-fouled decision point will likely be corrupted. The rate of bio-fouling varies widely, so we can not easily estimate how much data to discard. The sensor can go from clean to completely bio-fouled in as quickly as three weeks or as slowly as five months. Discarding some fixed number of days before the decision point would result in either loss of much clean data or retention of corrupted data. Consequently, we desire a fault detector that accurately estimates onset time.

Another critical problem is presented by the dearth of bio-fouling onset examples in the data archive. Developing Fisher LDA detectors require many fault examples. Unfortunately, all sensor stations in the estuary are missing onset examples for important periods of the year. Some sensors have been installed recently and have no bio-fouling examples whatever. A development approach that requires only clean example data would help alleviate this data shortage problem.

Finally, the above methods classify each measurement independently. However, human experts make bio-fouling judgements by watching the behavior of the salinity signal *over several weeks*. Likewise, we expect that using a method that accrues information over time will increase confidence in our bio-fouling decisions.

To address these issues, we introduce sequential likelihood ratio (SLR) tests. SLR tests combine several sequential measurements for every classification decision. They can be adapted to provide estimates of bio-fouling onset times. Finally, by defining a parameterized model of bio-fouling behavior, we can estimate the bio-fouling rate in real-time. Since we fit the fault model to the measurements under test, the classifier can be developed using only clean data examples.

6 Sequential Likelihood Ratio Tests

Sequential likelihood ratio tests accrue information to improve classification confidence [6]. The likelihood ratio for fault detection is the probability of a data measurement x assuming it is faulty, $\mathrm{p}(x|f)$, divided by the probability of x assuming it is clean, $\mathrm{p}(x|c)$. A likelihood ratio test compares the logarithm of this ratio to a threshold. If the value is above the threshold, the data is declared faulty. A *sequential* likelihood ratio test sums the log likelihood ratios over some time window and compares the sum to a threshold, λ, that is

$$h = \sum_{n=\tau}^{N} \ln \frac{\mathrm{p}(x_n|f)}{\mathrm{p}(x_n|c)} \underset{c}{\overset{f}{\gtrless}} \lambda \tag{7}$$

where the window begins at time $n = \tau$ and ends at current time N. If most of the data is faulty (clean), the sum will lie well above (below) the threshold and we will have high confidence in the classification decision. This framework can also be adapted to estimate the fault onset time. If we set the window length to maximize the log likelihood ratio, h, the best estimate of onset time is τ [8].

6.1 Bio-fouling Fault Model

In order to develop a sequential likelihood ratio test for bio-fouling detection, we first define models of the clean and bio-fouled data. We start with the model for salinity alone and latter add temperature. As before, md salinity s is modeled as a Gaussian signal with mean μ_s and variance σ_s^2. When the sensor is clean, it measures the true salinity value, so the measurement at time n is $x_n = s_n$. When the sensor bio-fouls, the measured value is suppressed relative to the true salinity. We model this suppression as a linear downtrend with rate (slope) m, that begins at time τ. The measured value becomes

$$x_n = g(n)s_n \tag{8}$$

where the suppression factor, $g(n)$, is

$$g(n) = \begin{cases} 1 & n < \tau \\ (1 - m(n - \tau)) & n \geq \tau \end{cases} \tag{9}$$

and m is the bio-fouling rate (1/sec). The probability density of measurement x_n is thus

$$\mathrm{p}(x_n) = \frac{1}{\sqrt{2\pi}g(n)\sigma_s} \exp \frac{-(x_n - g(n)\mu_s)^2}{2g^2(n)\sigma_s^2} \tag{10}$$

Both the measurement mean, $g(n)\mu_s$, and variance, $g^2(n)\sigma_s^2$, decrease as bio-fouling progresses.

Using these models for clean and bio-fouled salinity signals, we now write the SLR for md salinity. The values for the bio-fouling rate m and onset time τ are not known in advance, so we replace them with their maximum likelihood estimates. The SLR is

$$h = \max_{\tau,m} \sum_{n=\tau}^{N} \ln \frac{1}{1 - m(n - \tau)} + \frac{(x_n - \mu_s)^2}{2\sigma_s^2} - \frac{(x_n - (1 - m(n - \tau))\mu_s)^2}{2(1 - m(n - \tau))^2\sigma_s^2} \tag{11}$$

When a sequence of measurements fits the bio-fouled model better than the clean model, the second term in (11) is large and the third term is small, so h is positive. Consequently, when h is above a chosen threshold, the sensor will be classified as bio-fouled. The threshold is chosen to satisfy operational requirements. For this work, we choose thresholds so the classifiers have low false alarm rates.

Incorporating temperature information into SLR tests should improve classification accuracy. The appropriate SLR is the log probability of md salinity conditioned on temperature

given the bio-fouling model divided by the probability given the clean model. We start by modeling the salinity, s, and temperature-based mixing coefficient, α, as jointly Gaussian,

$$\mathrm{p}(s, \alpha) = \mathcal{N}(\mu, \Sigma) \text{ where } \mu = \begin{bmatrix} \mu_s \\ \mu_\alpha \end{bmatrix} \text{ and } \Sigma = \begin{bmatrix} \sigma_s^2 & \sigma_{s\alpha} \\ \sigma_{s\alpha} & \sigma_\alpha^2 \end{bmatrix}. \tag{12}$$

The probability of md salinity conditioned on temperature when the sensor is clean is Gaussian with $\mathcal{N}(\eta, \gamma)$, where the mean is the expected value of md salinity given temperature,

$$\mathsf{E}[s|\alpha] \equiv \eta = \mu_s + (\sigma_{s\alpha}/\sigma_\alpha^2)\,(\alpha - \mu_\alpha) \tag{13}$$

and the variance

$$\mathrm{var}[s|\alpha] \equiv \gamma = \sigma_s^2 - \sigma_{s\alpha}^2/\sigma_\alpha^2 \tag{14}$$

Since the temperature sensor is not susceptible to bio-fouling, we do not have to consider the case of both sensors degrading at the same time. When bio-fouling occurs, the salinity measurement is suppressed relative to the true value. Using the suppression factor $g(n)$ (9), the probability of the salinity measurement, x, conditioned on temperature is $\mathrm{p}(x_n|\alpha_n) = \mathcal{N}(g(n)\eta_n, g^2(n)\gamma)$. The SLR for salinity conditioned on temperature is then given by

$$h = \max_{\tau,m} \sum_{n=\tau}^{N} \ln \frac{1}{1 - m(n-\tau)} + \frac{(x_n - \eta_n)^2}{2\gamma} - \frac{(x_n - (1 - m(n-\tau))\eta_n)^2}{2(1 - m(n-\tau))^2\gamma} \tag{15}$$

When h is above our chosen threshold, the sensor is classified as bio-fouled.

6.2 Model fitting

The SLR classifier parameters, μ and Σ are determined from only clean example data; no bio-fouled examples are necessary. We find maximum likelihood estimates for these parameters from archival time series data. The mean values are given by

$$\mu = \frac{1}{N} \sum_{n=1}^{N} \begin{bmatrix} s_n \\ \alpha_n \end{bmatrix} \tag{16}$$

The salinity and temperature covariance matrix, Σ, is given by

$$\Sigma = \frac{1}{N} \sum_{n=1}^{N} \left(\begin{bmatrix} s_n \\ \alpha_n \end{bmatrix} - \mu \right)^T \left(\begin{bmatrix} s_n \\ \alpha_n \end{bmatrix} - \mu \right) \tag{17}$$

All other classifier parameter values, such as μ_s or $\mathsf{E}[s|\alpha]$, can be extracted or calculated from the mean vectors and covariance matrix.

To use SLR tests for bio-fouling detection, we determine the bio-fouled model parameters from the data under test and calculate h, (11) or (15), for the current time. At each time step, n, the onset time τ and bio-fouling rate m are fit by maximum likelihood methods to the past and current measurements. The SLR h is then calculated using these estimates. If h is above our threshold, the current measurement is classified as bio-fouled and the onset time is reported as τ.

Determining the onset time estimate, τ, requires searching over all past time for the SLR window length that maximizes the ratio, that is

$$\tau = \arg\max_{k} \sum_{n=k+1}^{N} \ln \mathrm{p}(x_n|f; m_{N-k}) - \ln \mathrm{p}(x_n|c). \tag{18}$$

where N is the current time and our notation m_{N-k} stresses that the bio-fouling rate is a function of the window length $N-k$. For each possible value for τ, that is $k = 3 \ldots N$, we first determine the maximum likelihood estimate for m_{N-k} (described below) and then calculate the corresponding SLR h_{N-k}. The estimated onset time, τ is the time k that gives the largest value of h.

For the salinity alone SLR, we find the maximum likelihood estimate of bio-fouling rate m, by setting the first derivative of (11) with respect to m equal to zero. This operation yields the relation

$$m \sum_{k=\tau+1}^{N} \frac{(k-\tau)^2}{\omega_k^2} \mu_s^2 = \sum_{k=\tau+1}^{N} \frac{k-\tau}{\omega_k} \left(\frac{(x_k - \mu_s)\mu_s}{\omega_k} - \sigma_s^2 + \frac{(x_k - \omega_k \mu_s)^2}{\omega_k^2} \right) \tag{19}$$

where $\omega_k = 1 - m(k-\tau)$ and N is the current time. Note that m appears both at the beginning of (19) and in the definition of ω, so we do not have a closed form solution for m. However, the ω values act as weights that increase the importance of most recent measurements. This weighting accounts for the expected decrease in measurement variance as bio-fouling progresses. To estimate m we take an iterative approach. First, initialize m to its minimum mean-squared error value given by

$$m^{(0)} = -\frac{\sum_{k=\tau+1}^{N} (k-\tau) \left(\frac{x_k}{\mu_s} - 1 \right)}{\sum_{k=\tau+1}^{N} (k-\tau)^2} \tag{20}$$

We obtain (20) by setting the bio-fouled variance equal to the clean variance in (11) and maximizing the resulting SLR. Second, repeatedly solve (19) for $m^{(i)}$ with ω calculated using the previous value $m^{(i-1)}$. The estimated rate value stops changing when h reaches a maximum.

For the salinity conditioned on temperature SLR, m is found by maximizing (15). The results are similar to (19) and (20) with μ_s replaced by η_k (13) and σ_s^2 replaced by γ (14). The classification procedure is the same as that for salinity alone SLR tests.

SLR tests address the limitations of our baseline classifiers. They provide an estimate of onset time by finding the time that the measurements switch from matching the clean model to matching the bio-fouled model. By parameterizing the bio-fouling model, we are able to develop the SLR test classifiers exclusively on clean example data. The bio-fouled model parameters are fit to the data under test. Finally, SLR tests classify a sequence of measurements, so that long salinity downtrends produce larger h values than do short downtrends. The strong response to sustained salinity decreases should increase our confidence in bio-fouling decisions.

7 SLR Test Evaluation

We evaluated classification accuracy, time to detection, and onset time accuracy of our SLR classifiers on CORIE test data. Classification accuracy is reported using ROC curves as in our earlier evaluations. Time to detection is the time difference between bio-fouling onset and the earliest time our classifiers correctly identify that the sensor is bio-fouled. We compare time to detection of all four classifiers to the time it takes a human expert to visually identify that the sensor is bio-fouled. For onset time evaluation, we simulated bio-fouled signals by applying a linear degradation function to clean salinity measurements. We compare the estimated onset time provided by our SLR classifiers with the known onset time.

7.1 Classifier Accuracy

We compared the classifier performance for our salinity alone SLR test, SLR(s), to the performance of the md salinity classifier discussed earlier. Figure 10 contains resubstitution and hold-out ROC curves for SLR classifier applied to Sand Island and Tansy Point data. The same curves for the md salinity classifier are shown in gray for comparison. Again we are interested in the classification accuracy at low false alarm rates due to the high cost of retrieving a sensor for cleaning. At Sand Island, the SLR classifier has accuracy comparable to or slightly lower than the the md salinity classifier when false alarm rates are low. At Tansy Point, the SLR classifier correctly labels more bio-fouled days when the false alarm

rate is below 10%. At the lowest threshold that gives no false alarms, the percentage of correctly labeled bio-fouled days increases from 40% to over 65%.

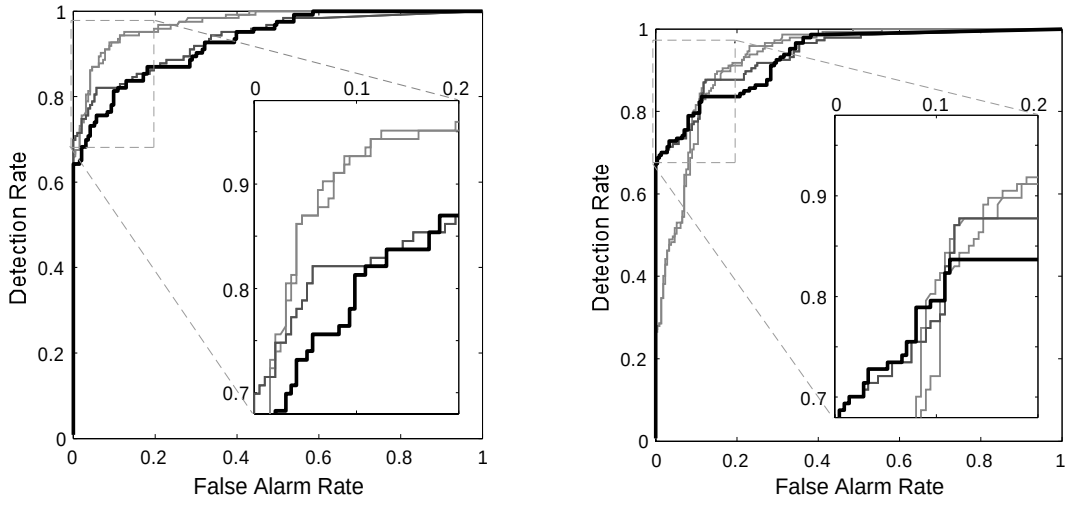

(a) Sand Island

(b) Tansy Point

Figure 10: Sequential likelihood ratio tests on maximum diurnal salinity. Resubstitution (thin line) and hold-out (thick line) ROC for classification of Sand Island and Tansy Point data. Maximum diurnal salinity results are shown in gray.

We also compared the classification performance of salinity conditioned on temperature SLR classifier, SLR($s|\alpha$), to the Fisher LDA classifier described earlier. The SLR classifier requires no fault example data to train the classifier, since fault parameters are fit to the data under test. One expects that classifiers developed using only clean or healthy data will have lower accuracy than classifiers developed using both clean and fault examples. However, at low false alarm rates, the SLR classifiers have accuracy comparable to the Fisher LDA classifiers. Figure 11 shows resubstitution and hold-out ROC curves for the salinity conditioned on temperature SLR test. The earlier results for the Fisher LDA classifier are shown in gray. For the Sand Island data, the SLR classifier is slightly less accurate than the Fisher linear discriminant when evaluated *on the training data*. However, the SLR classifier is more accurate for the more realistic hold-out tests. At Tansy Point, the SLR test classifies bio-fouled days at least accurately as the Fisher LDA classifier at 10% false alarms and more accurately at lower false alarms rates.

In summary, SLR classifiers for salinity alone are more accurate than the baseline md salinity classifier at low ($\leq$ 10%) false alarm rates. The SLR classifiers for salinity and temperature

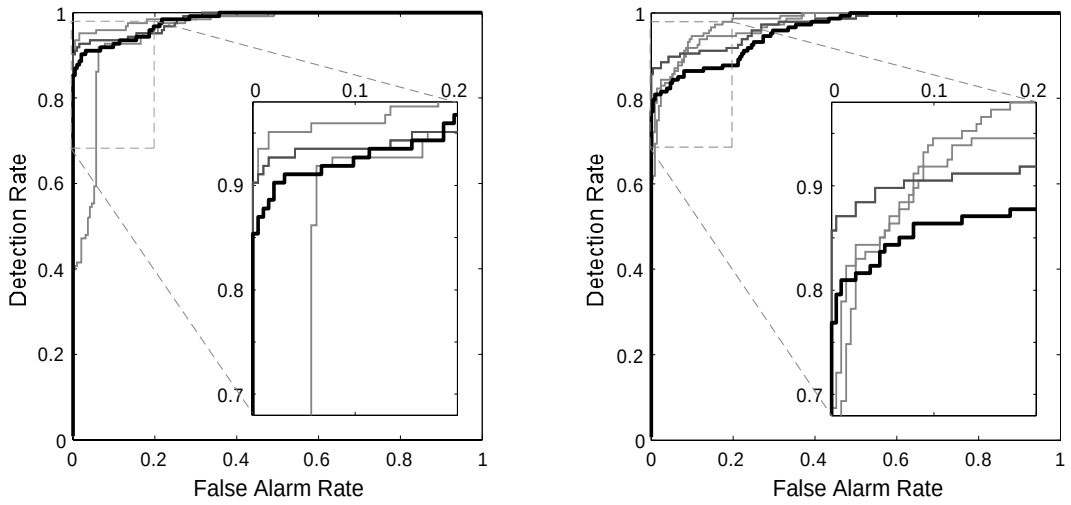

(a) Sand Island

(b) Tansy Point

Figure 11: Sequential likelihood ratio tests on maximum diurnal salinity conditioned on normalized temperature. Resubstitution (thin line) and hold-out (thick line) ROC for classification of Sand Island and Tansy Point data. Fisher LDA results are shown in gray.

are as accurate as Fisher LDA classifiers at low false alarm rates. As an added advantage, SLR classifiers achieve this accuracy without requiring bio-fouled training examples.

7.2 Detection Delay

Another way to evaluate our classifiers is to examine the time to detection. To minimize data loss and the real-time use of corrupted data, we need short times to detection. Since the exact time of bio-fouling onset is uncertain, we compare detection times relative to the onset times estimated visually by a human expert. We selected classifier thresholds to produce no false alarms on archival clean data. Detection time is the earliest time a discriminant exceeds and stays beyond the corresponding threshold. Included in our evaluation are a field scientist's estimates of when he would have scheduled a sensor to be cleaned, if he had monitored the salinity signal daily. We have very few bio-fouling onset examples; four for Sand Island and three for Tansy Point. To make the most use of limited data, all segments were used to both train the classifiers and evaluate detection time. Applying these classifiers and thresholds to new data may result in occasional false alarms.

site	segment	detection day				
	year	HE	Sal	SLR(s)	F LDA	SLR($s|\alpha$)
	1997	8	17	15	8	8
Sand	1999	4	16	16	7	5
Island	2000	9	11	9	4	4
	2001	15	17	15	9	9
Tansy	1999	74	59	30	23	9
Point	2000	11	13	16	11	12
	2001	9	†	†	10	10

Table 1: Estimated Bio-fouling Detection Times for Sand Island (top) and Tansy Point (bottom). Days are the number of days after onset time (as estimated by a human expert) that the classifier discriminant passed the no false alarm threshold. The HE column contains the day on which a human expert visually inspecting the sensor measurements estimates he would consider the instrument bio-fouled. For the classifiers, detection day is the earliest time that a discriminant passed and stayed beyond the no false alarm threshold. SLR(s) is SLR classifier for salinity alone, F LDA is the Fisher LDA classifier, and SLR($s|\alpha$) is the SLR classifier for salinity conditioned on temperature. † threshold not exceeded; this instrument was removed on day 12 to confirm bio-fouling indication by on-line Fisher LDA and SLR($s|\alpha$) classifiers.

Table 1 contains time of detection rounded to the nearest day for Sand Island and Tansy Point time-series segments. Since we have so few examples, we hesitate to make precise comparisons of detection time, but we do note a few general trends. Classifiers that incorporate both salinity and temperature measurements have detection times comparable to or a few days faster than the human expert. Classifiers based on salinity alone typically pass their thresholds several days after the field scientist estimates that he would identify bio-fouling.

To see how well our classifiers worked in practice, we implemented versions that operated on *real-time* salinity and temperature measurements. For all three instances of sensor degradation (two bio-fouling incidents and one instrument failure that mimicked biofouling) that occurred in the summer 2001 test period, our classifiers correctly indicated a sensor problem before the field staff was aware of it. In addition, the real-time classifiers produced no false alarms during the test period.

7.3 Onset Time Estimates

One advantage of sequential likelihood ratio tests is their ability to produce a maximum likelihood estimate of bio-fouling onset time. We would like to evaluate the accuracy of this estimate, but true onset times for our example data are not known. Instead of using actual bio-fouled examples, we generated simulated bio-fouled time series with degradation starting at a known time. The simulated time series consist of clean example data, x, where after the chosen onset time, τ the signal is linearly degraded until some minimum value is reached. The simulated signal y at time step n is thus

$$y_n = \begin{cases} x_n & n \leq \tau \\ (1 - m(n-\tau))\, x_n & n > \tau \text{ and } m(n-\tau) < 0.5 \\ 0.5\, x_n & \text{otherwise} \end{cases} \tag{21}$$

where m is the bio-fouling rate. We chose $m = 0.016/\text{sec}$, since rates measured from summer bio-fouling incidents ranged from 0.012 to 0.025. We classify the simulated bio-fouled data, y, and extract the onset time estimated when the discriminants first exceed their no false alarm thresholds.

Table 2 contains onset time estimates from the SLR classifiers for several example time series with simulated bio-fouling. In general, the onset estimates are within a day or two of true onset. There are a couple of exceptions worth noting. The first is illustrated by the Tansy Point example with onset day 8/14. In this case, the estimate from SLR(s) classifier is several days after the onset. There is a natural increase in salinity at the point where bio-fouling is applied, so salinity does not decrease until a few days after onset. The SLR($s|\alpha$) classifier uses temperature to recognize that salinity should have been increasing and gives a better estimate of onset time. The only problem found with the onset time estimate is illustrated by the Sand Island example with onset day 6/04. In this case, the estimate from both SLR classifiers is early. The md salinity measurements are below the expected value (either E[s] and E[$s|\alpha$]) for over a week before bio-fouling onset, so it fits the clean data model poorly. Hence, the SLR classifiers treat both the low md salinity data and the bio-fouled data as bio-fouled. We find that when bio-fouling occurs during or immediately following a period of low md salinity, the onset estimate is consistently too early.

site	segment year	onset day	SLR(s) onset	SLR(s) err	SLR($s\|\alpha$) onset	SLR($s\|\alpha$) err
	1999	6/07	6/07	0	6/06	− 1
Sand	1999	6/29	6/30	+ 1	6/30	+ 1
Island	2001	6/04	5/24	− 11	5/23	− 12
	2001	6/19	6/20	+ 1	6/20	+ 1
	2001	6/21	6/20	− 1	6/22	+ 1
Tansy	2001	7/02	7/05	+ 3	7/04	+ 2
Point	2001	7/13	7/15	+ 2	7/13	0
	2001	8/14	8/20	+ 6	8/15	+ 1

Table 2: Estimated bio-fouling onset times for Sand Island (top) and Tansy Point (bottom) Times are given as month/day. Onset day is τ in (21). The first degraded measurement occurs on onset day +1. Err is difference between estimated and true onset times. SLR(s) is the SLR classifier for salinity alone, and SLR($s|\alpha$) is the SLR classifier for salinity conditioned on temperature.

8 Discussion

The CORIE observation network includes measurements from CT sensors deployed throughout the Columbia river estuary. These sensors are subject to bio-fouling, that is the gradual degradation of sensor response due to the accumulation of biological matter on the sensor. To insure data integrity, we must detect this degradation within a few diurnal cycles of bio-fouling onset. In this paper, we described our successful initial efforts to develop automatic classifiers for these sensors. In this work, we concentrated on sensors subject to predominately hard-growth bio-fouling. However, we expect our methods to be most useful in detecting soft-growth bio-fouling, which is difficult to identify by visually examining the signal. In this final section, we summarize our work to date and discuss future plans to enhance our classifiers and develop bio-fouling detectors for sensors subject to soft-growth bio-fouling.

8.1 Summary

Prior to this work, no automatic bio-fouling detection existed for the CORIE salinity sensors. The field staff identify bio-fouling by periodic visual examination of the time series. Our initial work involved the development of two baseline classifiers, one which monitored maximum diurnal salinity and one based on Fisher linear discriminant analysis of salinity

and temperature. On the Tansy Point test data, the md salinity classifier correctly identified less than 30% of the bio-fouled measurements correctly at a detection threshold that produced no false alarms. The Fisher LDA classifier performed much better, identifying over 60% of the bio-fouled measurements correctly.

We also developed sequential likelihood ratio tests for salinity and salinity conditioned on temperature. These SLR classifiers have several advantages over our baseline classifiers; they accrue information over time to improve classification accuracy, they provide an estimate of bio-fouling onset time, and they do not require an extensive number of bio-fouled data examples to develop. On the Tansy Point test data, the SLR classifier for salinity alone correctly identified nearly 70% of the bio-fouled measurements correctly at a classifier threshold that produced no false alarms. Again incorporating temperature information improved classification performance as the SLR classifier for salinity conditioned on temperature correctly identified nearly 80% of bio-fouled measurements. This classification error rate corresponds to a delay between onset and detection that is comparable to or a few days faster than that of human experts. As an added advantage, the onset time estimates generated by the SLR classifiers are generally accurate to within a day or two of true onset time.

Our classifiers also performed well detecting sensor bio-fouling in real time. Classifiers deployed during summer 2001 detected all three epsisodes of sensor failure before the field staff noticed the signal degradation. In addition, these real-time detectors generated no false alarms during the test period.

8.2 Future Work

In developing the classifiers described in this paper, we assumed that md salinity measurements from clean sensors varied around some stationary mean value. However, in the spring and late fall, there are occasionally periods of depressed md salinity. At low false alarm rates, the measurements that are incorrectly identified as bio-fouled occur during these periods of low md salinity. In addition, the SLR classifier onset time estimates are consistently too early when md salinity is lower than expected. To correct these problems we plan to examine two possible solutions: model salinity with a mixture of Gaussian densities or adapt the model mean to the data under test.

One of our test cases indicates that our SLR classifiers may be effective in solving the difficult

problem of detecting soft-growth bio-fouling quickly. Most of the test cases presented in this paper were incidents of hard-growth bio-fouling. However, the 1999 time series segment from Tansy Point, Table 1, is a classic case of soft-growth bio-fouling with slow fitful degradation. Our expert did not identify bio-fouling on this segment until around seventy-five days after onset, much longer than his typical five to fifteen day delay. However, our SLR(s) classifier had a detection delay of around thirty days and the SLR($s|t$) classifier detected bio-fouling only nine days after onset. While we obviously can not draw conclusions from a single example, this test case encourages us to develop SLR classifiers for sites subject to soft-growth bio-fouling.

Developing bio-fouling detectors for sensors subject to soft-growth is complicated by the variability of salinity measurements at these stations. Soft-growth bio-fouling occurs predominantly up-river where there is less salt penetration than in the lower estuary. At these sensors, the md salinity measurement varies with the spring/neap tidal cycles of 14 and 28 days. This strong periodicity, with its frequent normal salinity decreases, makes it difficult to detect bio-fouling degradation quickly. We plan to investigate the use of time-series prediction to remove these normal salinity variations, which will facilitate development of SLR classifiers for accurate detection of soft-growth bio-fouling.

Acknowledgements

We thank members of the CORIE team, Arun Chawla and Charles Seaton, for their their help in acquiring appropriate sensor data and Michael Wilkin for his assistance in labeling the sensor data. We also thank Paul Hosom and Anna Farrenkopf for reviewing early drafts of this paper. This work was supported by the National Science Foundation under grant CCR-0082736.

References

[1] A. Baptista. Environmental observation and forcasting systems. In Meyers, editor, *Encyclopedia of Physical Science and Technology*. Academic Press, 2002.

[2] D. Steere, A. Baptista, D. McNamee, C. Pu, and J. Walpole. Research challenges in environmental observation and forecasting systems. In *Proceedings of the Sixth annual International Conference on Mobile Computing and Networking*, pages 292–299, 2000.

[3] A. Baptista, M. Wilkin, P. Pearson, P. Turner, C. McCandlish, and P. Barrett. Costal and estuarine forecast systems: A multipurpose infrastructure for the Columbia river. *Earth System Monitor*, 9(3), 1999.

[4] U.S. Army Corps of Engineers. Biological asssessment - Columbia river channel improvements project. Technical report, USACE Portland District, December 2001.

[5] G. Pickard and W. Emery. *Descriptive Physical Oceanograophy - An Introduction.* Pergamon Press, 1990.

[6] K. Fukunaga. *Introduction to Statistical Pattern Recognition.* Academic Press, 1990.

[7] C. Bishop. *Neural Networks for Pattern Recognition.* Oxford Press, 1995.

[8] M. Basseville. Detecting changes in signals and systems - a survey. *Automatica*, 24(3):309–326, 1988.